Reprinted from JOURNAL OF APPLIED PHYSICS, Vol. 40, No. 13, 5290–5300, December 1969
Copyright 1970 by the American Institute of Physics
Printed in U. S. A.

Periodic Potential Probe Configuration for Plasma Diagnostics*,†

EARL R. MOSBURG, JR.

National Bureau of Standards, Boulder, Colorado 80302

(Received in part 10 June 1968; in final form 2 June 1969)

A probe having a spacially periodic potential is created by a bifilar winding of small tungsten wire. This geometry results in an electric field configuration having an extremely short penetration distance into the plasma. When the behavior of this probe is studied in extended negative glow and back-diffusion type plasmas, the floating mode current–voltage characteristic curve is seen to be quite different from that of the usual double probe in that no effects of the electrons are observed. The behavior of the periodic probe is controlled by the ion inertia established in the diffusion region which lies just in front of the probe. The important parameter of the characteristic curve is the slope near zero applied voltage difference which can be related in a simple manner to the flux of plasma diffusing to the probe and to the diffusion drift energy of the ions as they reach the probe. The electrons make no contribution to this slope for low applied voltage differences. This probe thus provides a very sensitive method for measuring the diffusive flux of plasma to a containing wall.

I. INTRODUCTION

Contact probes of various types continue to provide a popular, although sometimes very frustrating, approach to the determination of electron density and temperature in a plasma. If a Langmuir probe is used, the electron temperature is determined from the shape of the probe characteristic curve near the ion current saturation, and the electron density usually from the electron saturation current.[1] In some plasmas, such as the extended negative glow,[2] a good electron saturation is not obtained. Furthermore, one is usually concerned about the perturbations produced by drawing large electron currents to the probe.

The double probe technique[1,3] minimizes the perturbation due to the probe, but the interpretation of ion current saturation in terms of electron density is not as clear. In both of these techniques, the field penetration into the plasma due to the potentials applied to the probes is not well defined and may depend on the applied potentials themselves. From another point of view the effective collecting area of the probe in the saturation region is an unknown, although slowly varying, function of the applied potentials and is therefore difficult to determine accurately. Because of the smallness of this collecting area, the sensitivity of the double probe is relatively low. Furthermore, the use of these probes in a magnetic field is extremely suspect due to the lack of a satisfactory theory for this case.

Recently in this laboratory we have been investigating the properties of a probe consisting of many very small parallel wires, closely spaced in a plane array. If alternate wires are connected to a common potential and the intermediate ones to a second potential, but floating with respect to the plasma, the result is a periodic configuration, as in Fig. 1(a), which exhibits some of the aspects of the usual double probe, but provides a high order multipole field with very short penetration distance.

The geometry under study consists of a boron nitride form measuring approximately 1.5×1.5×0.5-cm thick, the center of which has a clear aperture measuring 1×1 cm. Around this form is a bifilar winding of 0.0125-cm-diam tungsten wire, wound with 0.025-cm separation between wire centers so that the wires span the square aperture and are parallel to one edge. For some probes 0.005-cm wire was used at 0.010-cm center to center spacing.

It can be shown that the field penetration of such a configuration in the absence of plasma, is an exponential with an e-folding length less than the spacing between adjacent wires. This spacing can be made smaller than the mean-free path between electron-neutral collisions for pressures up to several Torr in helium. In helium at 1 Torr the m.f.p. is approximately 0.5 mm. To quite good accuracy the effective collecting area is determined by the total cross-sectional area provided by the electrodes in the array (cf. Sec. IV). This collecting area is relatively large thus assuring a rather high probe sensitivity. However, because of the large area of the electrodes, the periodic potential probe presents a large geometric perturbation to the plasma and is thus best considered as a wall probe. Indeed, operated in a floating mode, the periodic probe draws zero net current and therefore, at distances greater than a few e-folding lengths, appears like any other portion of an insulating wall. When such a probe is operated in floating mode in a helium extended negative glow plasma, the electron temperature cannot be derived from the probe curve, in direct contrast to the behavior of the usual double probe (cf. Fig. 2).

* This research was supported in part by the Advanced Research Projects Agency.

† Part of this research was carried out at the Electrotechnical Laboratory in Tokyo during the author's tenure of a Japanese Government Research Award.

[1] F. F. Chen, in *Plasma Diagnostic Techniques*, R. H. Huddlestone and S. L. Leonard, Eds. (Academic Press Inc., New York, 1965), Chap. 4, p. 125.

[2] K.-B. Persson, J. Appl. Phys. 36, 3086 (1965).

[3] E. D. Johnson and L. Malter, Phys. Rev. 80, 58 (1950).

II. BASIC THEORY OF THE MULTIPOLE POTENTIAL

The total electric field in the vicinity of the probe results from the combined effect of the impressed potential difference between the two electrodes of the probe and the space charge densities in the plasma. Since the space charge field associated with ambipolar diffusion to the wall results mainly from the space charge density located in the plasma proper rather than very near the probe, the contributions of applied field and ambipolar field are essentially decoupled. Therefore they can be calculated separately and then be superimposed to obtain the total field. We will now neglect the ambipolar field and calculate the applied field contribution using the Laplace equation, thus obtaining the maximum penetration distance of the applied field into the plasma. In principle, if the plasma density is sufficiently high, screening of the applied field by the plasma will be present and a solution of the Poisson equation will then be needed for any exact description of the field. The field penetration in this case will be less than for the Laplacian solution, which therefore represents the maximum field penetration from such a probe operated in a floating mode. The subject of screening and sheaths will be discussed further in Sec. IV. If this penetration length is sufficiently small, we will expect that the field between plasma and probe due to the space charge densities in the plasma proper will be, to first order, the same as that present between the plasma and any other section of an insulating boundary.

An exact solution of the Laplacian potential field for the case of cylindrical wire electrodes is quite complicated (cf. Appendix). Since the exact approach furthermore does not clearly exhibit the gross features of the solution, we will use a Fourier series approach in order to establish the $1/e$ penetration distance of the probe potential. For the case of cylindrical wire electrodes, this Fourier series method is not strictly correct, since separation of the equations in x and y is not possible; the coefficients c_n are functions of y. However, for a photoetched probe, where the electrodes have negligible extent in the y direction, the approach is valid and would lead to an exact solution if the correct coefficients, c_n, were known. This solution will still be approximately correct for the wire probe.

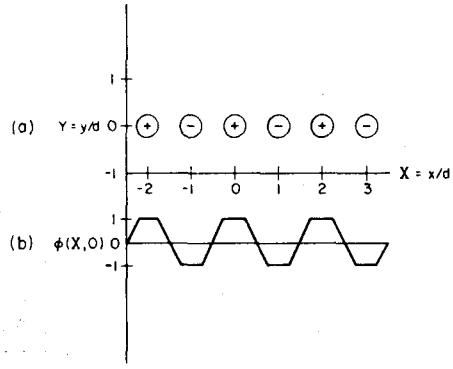

FIG. 1. Schematic cross section thru the top layer of wires in the periodic probe.

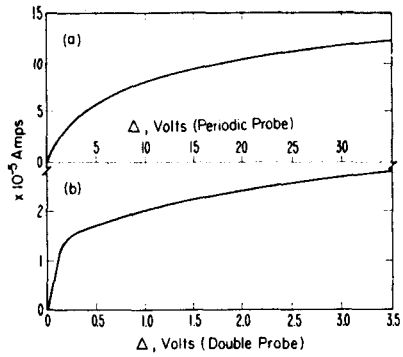

FIG. 2. Typical floating mode current vs voltage curves for (a) the periodic probe and (b) a normal double probe, for a helium extended negative glow discharge.

Let us then describe the electrostatic potential near the probe, in the total absence of plasma, by the expression

$$\phi(x, y) = \sum_{n=1}^{\infty} c_n f_n(y) \exp(inax), \tag{1}$$

where, as in Fig. 1, x is the coordinate along the array, perpendicular to the electrodes, and y is the coordinate perpendicular to the surface in which the array lies. With no further loss in generality we can set $f_n(0) = 1$, thus obtaining for $y = 0$

$$\phi(x, 0) = \sum_n c_n \exp(inax), \tag{2}$$

which is a Fourier series representation of the potential $\phi(x, 0)$, periodic in x. Substitution of Eq. (1) into the Laplace equation yields

$$\partial^2\phi/\partial x^2 + \partial^2\phi/\partial y^2 = 0 = -\sum_n c_n n^2 a^2 f_n(y) \exp(inax) + \sum_n c_n[\partial^2 f_n(y)/\partial y^2] \exp(inax).$$

For electrodes of infinitesimal extent in the y-direction this will hold if and only if

$$[\partial^2 f_n(y)/\partial y^2] = n^2 a^2 f_n(y) \quad \text{for all} \quad n. \tag{3}$$

Keeping in mind that $f_n(0) = 1$, we see that the solutions of Eqs. (3) are of the form

$$f_n(y) = \exp(-nay). \tag{4}$$

Then Eq. (1) becomes

$$\phi(x, y) = \sum_{n=1}^{\infty} c_n \exp(-nay) \exp(inax). \tag{5}$$

The periodicity in x for $\Delta x = 2d$, where d is the spacing between adjacent electrode centers of the probe, re-

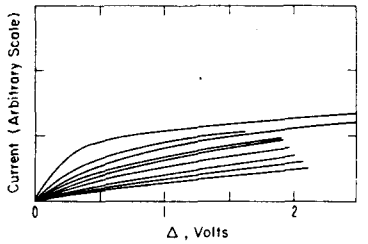

FIG. 3. Change in the shape of a double probe curve as the contamination of the probe surface increases.

quires that $a=\pi/d$. Thus the $1/e$ penetration distance of any given order potential term is given by

$$y=d/n\pi. \tag{6}$$

In order to calculate the potential $\phi(x,y)$, the appropriate coefficients, c_n, must be known. These coefficients depend on a knowledge of the form of the potential function $\phi(x,0)$, which itself can be exactly determined only thru the solution of an infinite series image problem. A good approximation to $\phi(x,0)$ is, however, the flat-topped triangular function of Fig. 1(b). Defining $A\equiv r/d$, where r is the electrode radius, and $X\equiv x/d$, $Y\equiv y/d$, Eq. (5) can be written in the form

$$\phi(X,Y)=\sum_{n=1} c_n \exp(-n\pi Y)\cos n\pi X, \tag{7a}$$

where

$$c_n=[8/n^2\pi^2(1-2A)]\cos n\pi A \quad \text{for odd} \quad n, \tag{7b}$$

and

$$c_n=0 \quad \text{for even} \quad n.$$

III. EXPERIMENTAL RESULTS

For the initial measurements a periodic probe was mounted flush with the wall of an extended negative glow helium plasma[2] for which the electron density, n, was about 3×10^{11} cm^{-3} and the electron temperature, kT_e, was approximately 0.07 eV. This discharge was operated in a tube of approximately 4-cm radius at gas pressures near 1 Torr (13.6 kg m^{-2}). Subsequently, extended negative glow discharges in neon and xenon at 0.1 Torr, $n\sim3\times10^{10}$ and 3×10^{11} cm^{-3} respectively, and in hydrogen at 0.2 Torr, $n\sim2\times10^{10}$ cm^{-3}, were used. In all cases when the probe is operated in floating mode as indicated in Fig. 4, one is immediately impressed by the total lack of a break in the current-voltage curve at a voltage near the electron temperature. In order to investigate the effect of surface impurities on the probe curve, a normal double probe[1,3] was operated in the same discharge. The striking difference between these two probe curves is illustrated for helium in Fig. 2.

With insufficient baking, the shape of the observed double probe curve changes drastically in the low voltage region following the termination of a cleaning procedure in which the probes are heated to red heat by electron bombardment. Immediately after cleaning, the double probe curve displays a sharp break which yields an electron temperature in rough agreement with previous spectroscopic measurements.[4] The shape then changes with time, yielding a progressively higher apparent temperature. This behavior is shown in Fig. 3. The time constant for this change in the shape of the probe curve is a measure of the relative impurity level in the discharge. With a relatively poor bake-out using heat lamps, a time constant of about 1 min was observed. As the bake-out procedure is improved the time constant is increased until finally, with overnight baking in an oven at approximately 400°C, the correct electron temperature is frequently obtained without further cleaning of the double probes, and the probe shape shows no deterioration with time over several hours.

In contrast to the above, curves of the periodic probe in these same discharge conditions exhibit no change in shape. The measured curve is totally independent of the impurity level indicated by the double probe and is also totally unaffected by resistively heating the wires to red heat prior to measurement. It is always similar to that shown in Fig. 2(a). In reference to Fig. 2, we will now describe the resulting curve as Type A or Type B depending on whether it resembles the periodic probe or double probe characteristic curve, respectively.

One possible explanation of this difference in probe behavior is that the curve of the periodic probe is produced by a surface leakage where the wires cross over the boron nitride form. Although the measured leakage resistance in the absence of plasma is greater than $10^{11}\,\Omega$, it is still possible that a surface charge layer may cause a greater leakage in the presence of a plasma. In order to measure such an effect, a special periodic probe was prepared having four interspersed, cylically ordered windings of wire on the boron nitride form. The wires thus appear in the order 1, 2, 3, 4, 1, 2, 3, 4, etc. If windings 1 and 3 are connected together and likewise windings 2 and 4, then the configuration is identical with that of Fig. 1 and the number of leakage paths is equal to the total number of wires minus one. If on the other hand, we connect windings 1 and 2 together and similarly windings 3 and 4, then the number of leakage paths is reduced by a factor of two. When this probe was operated in the same plasma in these two different ways, the curves coincided. We conclude from this that the surface leakage has a negligible effect on the characteristic curve of the probe.

We now consider the possibility that the observed behavior of the periodic probe might be due to a peculiar property of the extended negative glow plasma. In this plasma each ionization event is associated with an excess energy transfer from the electron beam of, on

[4] E. R. Mosburg, Jr., Phys. Rev. **152**, 166 (1966); R. S. Powers, Jr., Appl. Phys. **37**, 3821 (1966).

the average, 10 or 15 eV. It is conceivable that secondary electrons of this energy could be present in sufficient numbers to balance the ion current to the periodic probe and thus maintain a high floating potential. If the floating potential were so high that, for example, the thermal plasma electrons could not reach the probe, then a curve of Type *B* could not be observed. In order to investigate this possibility, measurements were made in the afterglow of a pulsed extended negative glow plasma. The curves remained of Type *A* indicating that secondary electrons are not responsible for the observed periodic probe behavior.

As an independent check on this, measurements in an entirely different type of plasma were desired and the periodic probe was therefore placed in the back-diffusion type plasma chamber of the Electrotechnical Laboratory in Tokyo, operated with helium and argon at pressures of 1.5×10^{-2} Torr ($0.204\ \mathrm{kg\ m^{-2}}$). This metal chamber has an inner diameter of 30 cm and a length of 80 cm. The back-diffusion type sources mounted axially at each end, produced electron densities ranging from 10^8 to $2\times10^9\ \mathrm{cm^{-3}}$ and electron temperatures kT_e, from 0.2 to 2 eV, depending on the mode of operation.

The results of these measurements are qualitatively the same as those in the negative glow plasma. Both periodic and double probe measurements were made. The probes were movable, although it was not possible to bring the probes any closer than approximately 5 cm from the wall of the plasma chamber.

The fact that such similar curves are observed in these two greatly different plasmas is a strong argument that the origin of the differences between periodic and double probe curves depends, not on any peculiar property of the plasma, but rather on the conditions in the vicinity of the probe which are imposed by the probe geometries.

As a help in understanding the difference between the periodic probe and double probe curves, another type of probe was made which has the small physical size of the double probe but the close wire spacing of the periodic probe. This probe is made of two wires 0.0125 cm in diameter and spaced 0.025 cm apart. The active length of the probe is approximately 0.5 cm. In reference to its geometry we have called it a "close dipole probe" (CDP). It was placed in the plasma with the wires parallel to the axis of the tube and was mounted in such a way that it could be moved smoothly in a radial direction between the center of the plasma and the wall.

TABLE I. Type of characteristic probe curve: *A* and *B* refer to Figs. 2(a) and (b); *H* or *L* indicate relatively high or low magnitude of probe floating potential. (The higher potentials indicate the presence of a diffusion sheath in front of the probe.)

Probe type	Probe location: Center	Probe location: Wall
Periodic probe	*A H*	*A H*
Close dipole probe	*B L*	*A H*
Double probe	*B L*	...

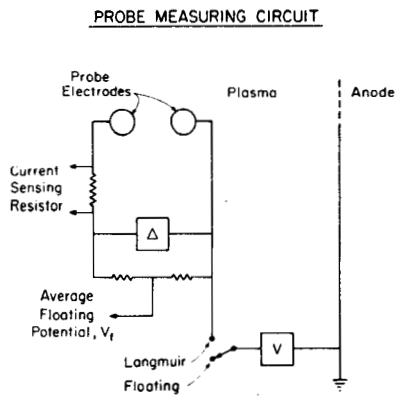

FIG. 4. Circuit diagram illustrating the floating mode and Langmuir mode measurements. In the Langmuir mode the voltage difference, Δ, is fixed and the voltage to ground, *V*, becomes the independent variable.

The results of many floating mode measurements made with these three types of probe are summarized in Table I. If, as is discussed in Sec. IV, the periodic probe curve is determined by the ion inertia imparted to the ions in the diffusion sheath region, then we would expect to observe exactly the behavior shown in Table I. Here the periodic probe is sufficiently large to create its own diffusion sheath, while both the double probe and the close dipole probe are much too small to do so. However, the movable CDP, which can be placed within 1 mm of the glass wall of the negative glow plasma, is able in this case to enter the diffusion sheath of the wall and thus measure a curve of Type *A*.

In addition to the floating mode measurements, the Langmuir mode was also used, in helium, as illustrated in Fig. 4. Typical current vs voltage curves for this type of measurement are shown in Fig. 5. Several important features are apparent. First of all, the ion saturation knee of the curves, from which the electron temperature can be calculated, is clearly visible in the periodic probe curves and yields values of $kT_e\sim0.07$ eV in agreement with values measured by other methods.[4] This is further evidence that surface impurities on the periodic probe are not a problem. A feature of the periodic probe curves which is not present in the double probe curves is the vertical shift which occurs when a constant voltage difference, Δ, is applied between the two electrodes. This vertical shift indicates that the two electrodes interact strongly with each other, that is, the sheath regions of the two electrodes overlap. Finally, the potential at zero current crossing, which is of course equal to the floating potential in the floating mode measurements, is quite distant from the knee of the curve. This indicates that electrons cannot con-

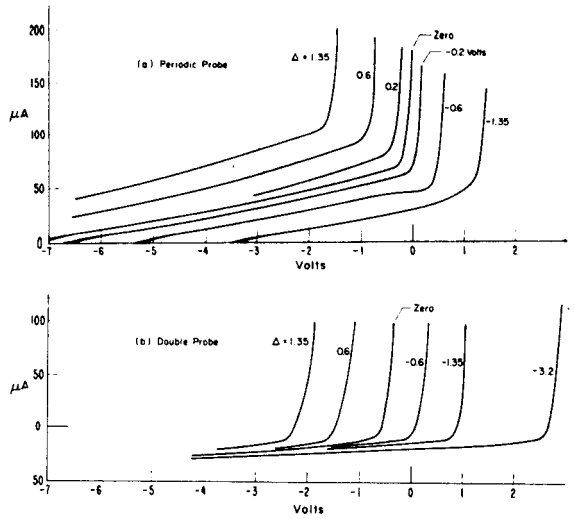

FIG. 5. Typical current vs voltage curves, in Langmuir mode, for (a) the periodic probe and (b) the double probe, for a helium extended negative glow discharge.

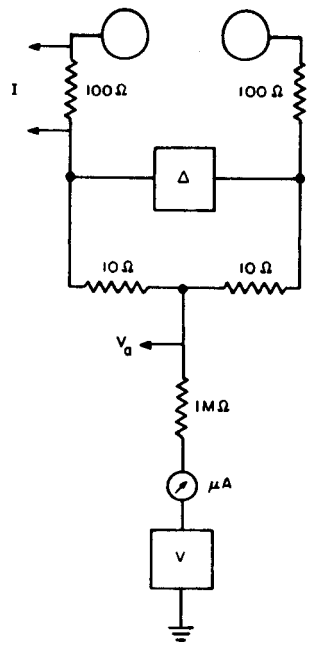

FIG. 7. Circuit diagram illustrating the periodic probe measurements with an imposed bias current.

tribute significantly to the characteristic curve of the periodic probe in floating mode. When similar Langmuir mode measurements are made with the CDP at the plasma center, we notice that the zero current crossing is at a low voltage, as for the double probe, but a very definite vertical shift is present, closely similar to the periodic probe curves.

When the probes are operated in floating mode and the floating potential, V_f, as indicated in Fig. 4, is measured as a function of the voltage, Δ, the resulting curves are those of Fig. 6. Here the periodic probe exhibits two distinct regions with transition occurring at about 10 V. The rapid increase in the magnitude of the potential V_f for values of Δ greater than 10 V is because in this region $\Delta/2 > (V_p - V_f)$ and the floating potential must increase like $\Delta/2$ in order to prevent the more positive of the electrodes from becoming positive relative to the plasma potential, V_p. This transition is probably responsible for the suggestion of a saturation which is noticeable in Fig. 2(a) at about 10 V. This rapid increase in floating potential above $\Delta = 10$ V is equivalent to an additional bias voltage which may effect a further perturbation of the plasma. The distinctive behavior of the periodic probe is to be found in the region $\Delta < 2(V_p - V_f)$, where the parameter of particular interest is the slope of the current–voltage characteristic curve at zero applied voltage, $dI/d\Delta$ at $\Delta = 0$. This will be discussed more fully in Sec. IV.

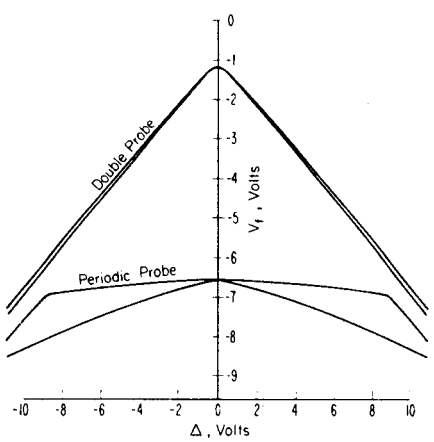

FIG. 6. Floating potential, V_f, of the periodic probe vs the applied voltage difference, Δ in a helium extended negative glow discharge. The voltage V_f is measured relative to the discharge anode. The two curves result from reversing the leads to the two probe electrodes thus showing the asymmetry in the contact of the plasma with the electrodes.

Using negative glow discharges in helium, xenon, neon, and hydrogen, and the back-diffusion plasma chamber with helium and argon, the flux determined

TABLE II. Values of the slope of the probe curve at $\Delta = 0$ and the average probe potential for different values of bias current.

Bias Current (μA)	V_a (V)	$dI/d\Delta$ at $\Delta = 0$ (Ω^{-1})
−150	−9.33	51.8×10^{-6}
−100	−8.09	55.5
−50	−6.86	58.8
zero	−5.83	62.2
+50	−4.85	67.3
+100	−3.89	72.0
+150	−3.07	76.6

from the periodic probe by the equation

$$\Phi_M = [k(T_i + T_e)/Ae^2\mathcal{A}_e]dI/d\Delta\,|_{\Delta=0}$$

was compared with the flux calculated from the known ion mobility by $\Phi_c = 760\mu_+ k(T_i + T_e)n/\Lambda p$, Λ being the diffusion length, p the gas pressure in Torr, and $\mathcal{A}_e$ the effecting collecting area of the periodic probe. These values generally show a correlation within a factor of about two over a range of Φ values equal to approximately 200. Considering the uncertainties in the parameters involved, this is a reasonably good correlation between the two sets of Φ values.

In order to experimentally verify the lack of influence of electrons on the slope of the characteristic curve, a further test was made using the circuit shown in Fig. 7 so that a bias current is drawn through a high resistance, coupled symmetrically to the periodic probe. If the bias current is made higher than the current calculated by multiplying the electronic charge into the calculated ambipolar flux of plasma to the probe, we can then be fairly certain that no electrons are reaching the probe. The behavior of the measured slope of the characteristic curve for different bias currents is shown in Table II for helium at 1.4 Torr. Since $n = 9.4\times 10^{11}$ cm^{-3}, $\Lambda = 1.69$ cm and $k(T_i + T_e) \approx 0.13$ eV, we obtain a value of $\Phi_c = 4.1\times 10^{14}$ cm^2 sec^{-1}. Assuming the probe area to be 1 cm^2, the corresponding current, $e\Phi_c A = 66\ \mu$A. The slope for zero bias current yields a value $\Phi_M = 2.0\times 10^{14}$ cm^{-2} sec^{-1} which compares well with the value of Φ_c above.

A bias current of between -50 and $-100\ \mu$A, which should result in the elimination of any electron contribution to the probe characteristic curve, results in a decrease in the slope by only 6% to 12%. Therefore we must conclude either that the electron contribution to the measured circulating current exhibits a slope essentially the same as that for the ions (a rather unlikely conclusion), or that the electron contribution to the current is negligible. A theoretical argument in support of this latter conclusion will be given in Sec. IV.

The slight changes in the measured slope as indicated in Table II are consistent with slight changes in the drift energy of the ions due to changes in the potential V_a. Thus as V_a becomes more negative we would expect the ion drift energy, at the probe, to increase slightly. The ions would then be harder to deflect and the measured slope would decrease as observed.

IV. FURTHER THEORETICAL CONSIDERATIONS

We turn now to consider the probable sheath conditions when the inequality $\lambda \ll r \ll L$ is valid. Here λ is the Debye length; r, the radius of the probe electrode; and L, the electron-neutral or ion-neutral mean-free path. For a small floating probe in such a situation, it can be argued that an effective electrostatic sheath thickness smaller than the radius of the probe is not possible. In essence this argument can be presented as follows. In the following we consider the plasma potential far from the probe to be zero and measure all other potentials with respect to it. Starting now at the probe, which has a potential of magnitude $|V_p|$, and proceeding outward, we find that the magnitude decreases in some monotonic manner. For our purposes we will define the effective sheath edge as that point where the magnitude of the potential reaches a value, $|V_s|$, small enough to present only a negligible perturbation to the particles in the free plasma some distance away. Thus

$$e\,|V_s| \ll kT_i, \tag{8a}$$

and

$$e\,|V_s| \ll kT_e. \tag{8b}$$

Unless the probe potential is very close to the plasma potential, we also have the condition $|V_s| \ll |V_p|$.

We now assume that this sheath thickness is much less than the probe radius and consider the consequences when the probe potential is negative relative to the plasma. Since the perturbation is assumed negligible, the flux and density of the attracted particles, the ions, at the sheath edge will be[1]

$$\Phi_i = n\bar{v}_i/4, \tag{9a}$$

$$n_i = n/2. \tag{9b}$$

On the other hand the flux and density of the repelled particles, the electrons, which are assumed to have a Maxwellian distribution, are given by

$$\Phi = n\bar{v}_e \exp(-eV_s/kT_e), \tag{10a}$$

and

$$n_e = n \exp(-eV_s/kT_e). \tag{10b}$$

Because $|V_s|$ is by definition very small, there must be quasi neutrality and hence $n_e \approx n_i$ at the sheath edge. But the equality of Eqs. (9b) and (10b) for the densities, can be satisfied only if

$$eV_s \approx kT_e \ln 2. \tag{11}$$

Because of the inequality (8a), we arrive at the requirement that

$$kT_i/kT_e \gg \ln 2, \tag{12}$$

a condition that cannot be satisfied for the plasmas we are considering where $T_e \gg T_i$.[5] If the sheath edge is now allowed to expand outward so that the sheath thickness is of the order of the probe radius, then the solid angle blocked by the probe decreases and n_i increases and can be expressed as

$$n_i = n/c, \tag{13}$$

where $2 < c < 1$. Equation (12) then becomes

$$kT_i/kT_e \gg \ln c, \tag{14}$$

[5] For a positive probe, T_e and T_i are reversed in Eq. (12) and the inequality can then be true for common plasmas.

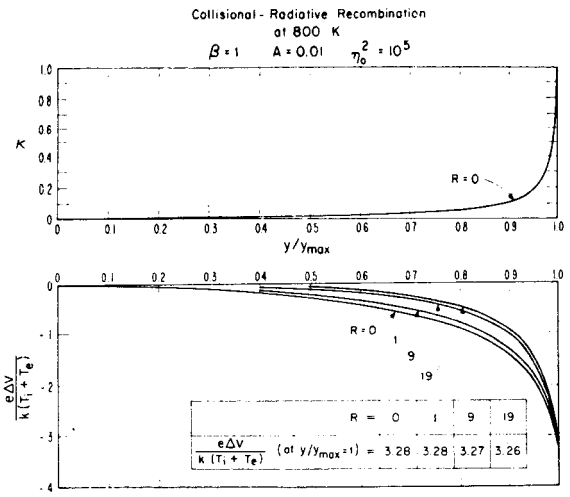

FIG. 8. Curves of the normalized plasma drift velocity

$$\kappa = u/[k(T_i+T_e)/M]^{1/2}$$

and the plasma potential $e\Delta V/k(T_i+T_e)$ vs the radius parameter y/y_{max} are given for different values of R, the ratio of recombination loss rate to diffusion loss rate at the plasma center. The notation is that of Ref. 8. The curves are for an extended negative glow discharge.

which can be satisfied for c sufficiently close to unity, even when $T_e \gg T_i$.

Since, as shown above, the electrostatic sheath around a negative probe must of necessity be at least the order of the probe radius in size, then it is clear that when such probes are placed a probe diameter apart, as for the periodic probe configuration, the sheath regions will be overlapping to some extent. The observed vertical shift of the Langmuir mode curves (described in Sec. III and Fig. 5) provides experimental confirmation of this effect. It should be noted that the penetration distance of the multipole potential, given by Eq. (6) is then less than the size of such a sheath. The periodic potential probe can therefore be considered as a geometry for which both electrodes are immersed in a common sheath.

For such a large probe the perturbation to the plasma is quite large. In fact if the probe is much larger than the mean-free path, it acts to a large extent like a section of the confining wall. This effect can be increased by mounting the probe so that its face is flush with the wall of the plasma container. In such a case, a well developed diffusion region, or diffusion sheath, will be present under ambipolar flow conditions. This diffusion region is, to a large extent, a bulk plasma phenomenon and the associated space charge field penetrates the whole plasma.

We will now consider the conditions in the plasma at some small distance from the periodic probe, such as $y \sim 2d$, where we are well outside of any inner sheath and where the effect of the applied multipole potential is negligible. We now ask to what extent the ion drift energy is developed in this region.

At the boundary itself the approximate ion drift energy can be obtained by applying the Bohm criterion[6] which requires that this energy be $k(T_i+T_e)/2$. However, if the space charge field producing this drift were confined to a sheath region very close to the boundary, then we would not necessarily expect the ion drift energy to be large in the region near $y=2d$. By solving the complete nonlinear diffusion equations[7] the drift velocity can be obtained as a function of radius within the plasma container, with the Bohm criterion automatically satisfied at the boundary. These equations can be modified to include the case of the extended negative glow discharge and the effect of volume recombination.[8] The plasma potential, V, and its corresponding dimensionless parameter, $\mho$, can be calculated as a function of radius, by means of the equation

$$\mho = e(V_c - V)/k(T_i+T_e)$$
$$= \tfrac{1}{2}\kappa^2 + \gamma^{-1}\int_0^y \kappa dy + (\beta+1)\int_0^y (\kappa^2/y)dy, \quad (15)$$

where V_c is the value of V at the plasma center. The other symbols are defined in Ref. 8. Typical curves of $\mho$ and κ, the ion drift velocity normalized to $[k(T_i+T_e)/M]^{1/2}$, are given in Fig. 8 as a function of the radius parameter y/y_{max}. Similar curves of κ vs y/y_{max} are given for a positive column type discharge in Ref. 7. Notice in Fig. 8 that the variation in potential is not confined to a small sheath region near the boundary but penetrates deep into the plasma, and that the ion drift velocity is well developed long before the plasma reaches a region as close to the boundary (or the periodic probe) as that specified by the distance $y \sim 2d$, which for our plasma corresponds to about 1% of the tube radius or less. We will therefore assume that, within this distance $y \sim 2d$, the ion drift energy is equal to the value expected at the plasma boundary and will proceed to investigate the consequences of this assumption.

Since the net outward particle fluxes for a floating probe are equal for the electrons and ions, it is clear that the outward mass flow, or momentum, is in the ratio of the particle masses. The flow is therefore completely dominated by the ion inertia. Since the ion drift energy, $k(T_i+T_e)/2$, is considerably larger than the value of kT_i, and since the multipole potential does not penetrate into the plasma, the situation at a distance $y \sim 2d$ from the probe surface can be fairly accurately represented by assuming a uniform, monenergetic ion beam of energy V_0 incident normal to the plane of the probe. Since the penetration distance of the multipole potential applied

[6] D. Bohm, in *Characteristics of Electrical Discharges in Gases*, A. Guthrie and R. K. Wakerling, Eds. (McGraw-Hill Book Co., New York, 1949), Chap. 3.

[7] K.-B. Persson, Phys. Fluids **5**, 1625 (1962); E. R. Mosburg, Jr. and K.-B. Persson, Phys. Fluids **7**, 1830 (1964).

[8] E. R. Mosburg, Jr., Phys. Fluids **9**, 824 (1966).

to the probe, Eq. (6), is less than the distance from an electrode needed to establish any effective sheath potential, we can therefore calculate the ion trajectories to first order using the Laplacian potential, Eq. (7), in a collisionless theory. Referring to Fig. 1(a), we see that the problem can be simplified to that of a single cell defined by the symmetry planes at $x=0$ and $x=1$. We now consider the ions reaching each electrode with grazing trajectories as shown in Fig. 9.

We will consider the case of thin flat electrodes, rather than cylindrical wire electrodes, since Eq. (7) can be used to describe the potential close to such electrodes. The equations of motion of the ions in dimensionless form are then:

$$\dot{X}=-\tfrac{1}{2}(\partial V/\partial X) \qquad \ddot{Y}=-\tfrac{1}{2}(\partial V/\partial Y), \tag{16}$$

and V is expressed, using Eq. (7), as

$$V=D\sum_{\text{odd } n}[8\cos n\pi A/n^2\pi^2(1-2A)] \times \exp(-n\pi Y)\cos n\pi X. \tag{17}$$

Here we have used the definitions of X, Y, and A as in Eq. (7), $T\equiv v_0t/d$, $V\equiv e\phi/\frac{1}{2}Mv_0^2$, and $D\equiv(e\Delta/2)/\frac{1}{2}Mv_0^2$, where v_0 is the incident velocity of the ions entering the multipole field of the probe.

Since we are assuming a monoenergetic, normally incident ion beam, there will be no crossing of ion trajectories, and therefore the calculation of the two trajectories which strike the edges of the two electrodes in Fig. 9 is sufficient to determine the ion currents to these electrodes. Since we desire only the slope of the characteristic curve near $\Delta=0$, these trajectories have a nearly constant value of $X\approx A$ so that we may take $X=A$ in evaluating the force, $-\partial V/\partial X$, acting on the ion. Furthermore the retardation of the ions is negligible to first order so that $\dot{Y}\approx\text{constant}=-1$ along the trajectory. With these two approximations we may write

$$\dot{X}=-\frac{1}{2}\int\frac{\partial V}{\partial X}dT=-(2\dot{Y})^{-1}\int_{\infty}^{Y}\frac{\partial V}{\partial X}dY. \tag{18}$$

Integrating again we obtain

$$\Delta X=-\frac{1}{2\dot{Y}^2}\int_{\infty}^{0}\left(\int_{\infty}^{Y}\frac{\partial V}{\partial X}dY\right)dY. \tag{19}$$

Taking the partial derivative, $\partial V/\partial X$, of Eq. (17), substituting into Eq. (19), and remembering that $\dot{X}=0$ as $Y\to\infty$

$$\Delta X=\tfrac{1}{2}D\sum_{\text{odd } n}^{\infty}[8\cos n\pi A/n^3\pi^3(1-2A)]\sin n\pi X. \tag{20}$$

Referring again to Fig. 9, we see that the ion flux to the electrode at potential $+D$ is given by $\Phi(A-\Delta X)$ and to the electrode at $-D$ by $\Phi(A+\Delta X)$. The total ion flux to the electrodes of both potentials, given by the sum of these expressions, is therefore $\Phi A/2$ and is

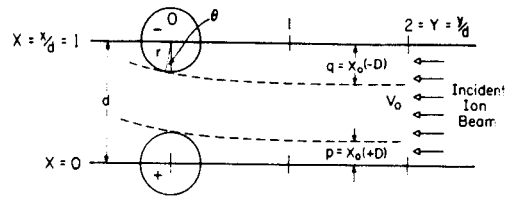

FIG. 9. Ion trajectories in one symmetry cell of the periodic probe.

independent of the applied potential, D. The effective collecting area of the probe is therefore unchanged. The measured circulating current of the probe, obtained from the difference of these fluxes multiplied by the electronic charge, is $I=2e\Phi\Delta X$. Defining the dimensionless current variable as $\mathcal{I}\equiv I/\Phi_e$, where Φ is the incident ion flux (ions cm^{-2} sec^{-1}), and using Eq. (20) with $X=A$, we see that

$$d\mathcal{I}/dD=[2/(1-2A)]\sum_{\text{odd } n}^{\infty}(2\sin 2n\pi A/n^3\pi^3). \tag{21}$$

The summation of this infinite series[9] can be obtained after we have noticed, defining $n=2m$, that

$$2\sum_{\text{odd } n}[\sin 2n\pi A/(2n\pi)^3]=2\sum_{n}-2\sum_{\text{even } n}, \qquad n>0,$$

and

$$2\sum_{\text{even } n}[\sin 2n\pi A/(2n\pi)^3]=\tfrac{1}{4}\sum_{m}[\sin 2m\pi(2A)/(2m\pi)^3], \qquad m>0. \tag{22}$$

The final result of this manipulation of Eq. (21) is the simple result

$$d\mathcal{I}/dD=A. \tag{23a}$$

Eliminating the dimensionless variables in favor of the observed variables, this becomes

$$dI/d\Delta=(\Phi e/2V_0)A=(n_0e^2/Mv_0)A, \tag{23b}$$

where $eV_0=\frac{1}{2}Mv_0^2$ is the energy of the incident ions expressed in electron volts, and n_0 is the density of the incident ion beam just before entering the multipole field of the probe.

There are two checks on the validity of Eq. (23). Since the ions are moving in a noncentral force field, angular momentum is not strictly a conserved quantity. However, when the potential difference, Δ between electrodes is very small, the force on the particle having impact parameter p (cf. Fig. 9) due to the electrode at $x=0$ is much greater than the force due to the electrode at $x=1$. In this case the angular momentum of each particle about the near electrode is still approximately conserved. When energy and angular momentum in such grazing trajectories are assumed to be rigorously conserved, we again obtain Eq. (23) in a simple and

[9] L. B. W. Jolley, *Summation of Series* (Dover Publications Inc., New York, 1961), p. 106, Series No. 574.

direct manner. A more accurate check is obtained from a solution of the equations of motion, Eqs. (16) and (17), on a CDC 3800 computer. The computed slope at zero voltage agrees with Eq. (23) within the 0.1% accuracy of the calculation. Furthermore the deviation from this slope is less than 2% for values of $D\equiv(e\Delta/2)\frac{1}{2}Mv_0^2$ less than 0.5.

When the probe electrodes have appreciable extent in the y direction, as for the wire-wound periodic probe, the potential will be different from that given by Eq. (7) and some modified form of Eq. (23) will be needed to describe the slope at $\Delta=0$. The calculation for the case of electrodes with circular cross section is treated in the Appendix.

So far in this section we have said nothing about the contribution of electrons to the measured probe current. However, the experimental data indicate that the electrons do not provide a significant contribution to this current. As will now be shown, it is possible to understand this within the concept of the periodic probe developed thus far for thin flat electrodes.

The average density of ions at the surface of an electrode is dependent on two effects: (1) the deflection of ions thru an amount $\Delta X(X)$ which spreads the ion trajectories and thus reduces the density as D increases and (2) the reduction in speed of the ions produced by a potential $D>0$ which increases the density. It will now be shown that these two effects cancel to first order in the limit of small D.

If all ions were deflected by an equal amount, then, neglecting retardation, the density at the plane of the probe would be unchanged. If, however, as indicated by Eq. (20), this deflection is a function of X, then the density will be modified by an amount proportional to the rate of change of ΔX with X,

$$n/n_0=1-(d/dX)\Delta X, \tag{24}$$

where n_0 is the density in the incident, undeflected beam. In order to satisfy the continuity requirement, neglecting deflections for the moment, we must require that $n\dot{Y}\ (Y=0)=n_0\dot{Y}\ (Y=3)=-n_0$, since $\dot{Y}\ (Y=3)=-1$.

Now combining these deflection and retardation effects and averaging the density over the plane $Y=0$ from $X=0$ to $X=A$, we obtain

$$\langle n\rangle/n_0=(A\dot{Y})^{-1}\int_0^A[1-d(\Delta X)/dX]dX, \tag{25}$$

and hence

$$\langle n\rangle/n_0=[A-\Delta X(A)]/A\dot{Y}. \tag{26}$$

Summing Eq. (20) as before,[9] we obtain the expression $\Delta X(A)=AD/2\dot{Y}^2$. From conservation of energy considerations $\dot{Y}^2\ (Y=0)=1-D$, hence $\dot{Y}\approx 1-(D/2)$ for small D. Substituting these expressions into Eq. (26) we see that $\langle n\rangle/n_0$ is unity to the first order in D. Thus the effect of small values of D is to change the flux of ions striking an electrode without changing the average ion density at its surface.

The ion density at the plasma boundary can be estimated by noting that the product of this density with the plasma drift velocity $[k(T_i+T_e)/M]^{1/2}$ must equal the measured or calculated fluxes given by Φ_M or Φ_c in Sec. III. Although this calculation leads to a value of the ion density lower by about two orders of magnitude than the density at the plasma center, it is still sufficiently high ($\sim 10^9$ cm^{-3}) that the approximate equality $n_i\approx n_e$ is valid. The Debye length in this case is approximately 5×10^{-3} cm. Since many electrons of very low energy are present near an electrode, this equality of n_i and n_e can be maintained by changes in the local space potential which are very small compared to the voltage difference applied between the probe electrodes.

Since the plasma diffusion drift velocity is much less than the electron thermal velocity, and since the electrons are repelled by the probe, the electron velocity distribution near the probe electrode remains sensibly Maxwellian. The electron temperature in such a case is unmodified by changes in the repelling potential. Since both the electron density and the electron temperature are unchanged by the presence of small D, the electron flux, $n_e\bar{v}_e$, to a probe electrode must also be constant. There is therefore no contribution by electrons to the measured probe current when small difference voltages are applied to the electrodes. This conclusion is supported by the experimental data described near the end of Sec. III.

V. CONCLUSIONS

The periodic potential probe may provide a useful new tool for the measurement of the ambipolar flux of a plasma to its confining wall. It is particularly useful for the measurement of low fluxes since the size of the periodic probe can in principle be made arbitrarily large. The important parameter is the slope $dI/d\Delta$ of the characteristic curve at $\Delta=0$ [cf. Eq. (23)]. Because this parameter is determined entirely by the ions with no significant contribution from the electrons, and because the field penetration is so low, we expect that the behavior of the periodic probe can be described by this theory even in the presence of substantial magnetic fields. Since the response of the probe also depends on the drift energy with which the ions approach the probe, it may be possible to use it, in a situation where the ambipolar flux can be accurately calculated, in order to determine whether or not the Bohm criterion is actually satisfied in the boundary region. Some recent calculations[10] have indicated that this criterion is not always valid.

---

[10] P. N. Hu and S. Ziering, Phys. Fluids 9, 2168 (1966); H. A. Hassan, Phys. Fluids 11, 1085 (1968).

Finally it should be pointed out that other techniques for creating the periodic geometry should be possible. We have experimented with a probe consisting of two interlocking comb-shaped electrodes, photoetched on a small pyrex plate. This array was 1 cm^2 and consisted of about 200 conducting lines and 200 spaces. Although the operation of this type of probe has not yet proved satisfactory, efforts in this direction are continuing.

ACKNOWLEDGMENTS

The author wishes to thank Franklin B. Haller for contributions to the design and construction techniques of the periodic probes and Dr. Karl-Birger Persson for the basic idea of a charge separating probe and for many helpful discussions during the early part of the work. Thanks are due to the Japanese Government for the Research Award and to the Electrotechnical Laboratory for making possible my work there. The help of the members of the Plasma Section is gratefully acknowledged and special thanks are due to Satoru Kiyama and Hiroko Shimahara for assistance with the measurements in the back-diffusion plasma. Finally the author wishes to acknowledge the skillful computer programming carried out by Mrs. Bernice K. Bender.

APPENDIX

The potential surrounding an infinite grating of wires of circular cross section can be calculated by a Schwartz–Christoffel transformation as indicated by Richmond.[11] Since none of the three cases treated in this reference are identical to that of interest here, we will outline the modified method used to calculate our case.

As in Ref. 11, the relation between the complex position coordinate, z, and a complex parameter, t, is given by

$$dz/dt=\{P/[(t-1)t]^{1/2}\}+\{Q/[(t-a)t]^{1/2}\}. \quad (A.1)$$

This can be integrated to give the relation

$$z=2P \text{ arc tanh}[1-(1/t)]^{1/2}+2Q \text{ arc tanh}[1-(a/t)]^{1/2}, \quad (A.2)$$

where $z=A$ when $t=a$, $z=-iA$ for $t=1$, and $z=-i/2$ for $t=0$. It then follows that the parameter, a, can be determined from the equation

$$\{1/\text{arc tanh}[1-(1/a)]^{1/2}\} +[1/\text{arc tan}(a-1)^{1/2}]=1/\pi A, \quad (A.3)$$

and that

$$P=A/2 \text{ arc tanh}[1-(1/a)]^{1/2}, \quad (A.4)$$

and

$$Q=A/2 \text{ arc tanh}(a-1)^{1/2}. \quad (A.5)$$

As before, A is the ratio of the electrode radius to the distance between the centers of adjacent electrodes. The coordinate z is related to our position coordinate, $Z=X+iY$, by the relation $z=-iZ$.

For our case, the derivative dW/dt of Ref. 11 becomes

$$dW/dt=1/[(t-1)(t-a)t]^{1/2} \quad (A.6)$$

which integrates to give

$$W=F[\phi \mid (1/a)]/K(1/a) \quad (A.7)$$

where F and K are incomplete and complete elliptic integrals[12] respectively, and $\phi=\text{arc tan}[a/(t-a)]^{1/2}$.

When the value of t, determined from Eq. (A.2) for a given value of Z, is substituted into Eq. (A.7), the real part of W is the value of the potential. In Table III we have compared the behavior of the potential for $X=A=0.25$ and its derivative $\partial V/\partial X$ for circular and flat electrodes. For values of $Y>1$ both V and $\partial V/\partial X$ are proportional to $\exp(-\pi Y)$, although the proportionality constant differs by a factor of 1.832 for the two cases. This noticeable difference leads to different calibration factors when Eq. (19) is evaluated.

TABLE III. Values of the potential and its derivative for circular and flat electrodes for $X=A=0.25$.

	Circular electrode		Flat electrode		Ratio circular/flat	
Y	V	$\partial V/\partial X$	V	$\partial V/\partial X$	V	$\partial V/\partial X$
0.02			0.886	1.916		
0.04	0.986	5.035	0.808	1.842	1.220	2.733
0.06	0.970	4.883	0.743	1.760	1.306	2.744
0.08	0.947	4.674	0.687	1.684	1.378	2.776
0.1	0.918	4.420	0.637	1.606	1.441	2.752
0.2	0.737	3.004	0.448	1.248	1.645	2.407
0.4	0.415	1.403	0.233	0.706	1.781	1.987
0.6	0.224	0.719	0.123	0.384	1.821	1.872
0.8	0.1201	0.3795	0.0657	0.2061	1.828	1.841
1.0	0.0641	0.2018	0.0350	0.1101	1.831	1.833
2.0	0.00277	0.0087	0.00151	0.00476	1.832	1.832

[11] H. W. Richmond, Proc. Lon. Math. Soc. Ser. 2 **22**, 389 (1923).
[12] L. M. Milne-Thomson, *Handbook of Mathematical Functions*, M. Abramowitz and I. A. Stegun, Eds. [Natl. Bur. Stand. Appl. Math. Ser. 55 (1964)], Pt. 17.

TABLE IV. Effective values of A to be used in Eq. (23) for different electrode geometries.

	$A=0.15$	$A=0.25$	$A=0.35$
Flat electrodes	0.15	0.25	0.35
Circular electrodes	0.252 ($=1.68A$)	0.505 ($=2.02A$)	0.929 ($=2.65A$)

The values of the potential for circular electrodes were checked by repeating the calculation for values of $A \leqslant 0.01$ where comparison could be made with the more simple theory for vanishingly small A. As a final test, with $A=0.25$, the potentials for both the circular and flat [Eq. (7)] electrode cases were checked by actual measurements using conducting paper on which the appropriate geometries were painted with silver paint.

We therefore conclude that the factor, A, in Eq. (23) for the slope at $\Delta=0$, is geometry sensitive. In the case of circular electrodes, it must be replaced by the factors calculated using the proper values of $\partial V/\partial X$ in Eq. (19) and tabulated in Table IV.